

Synthesis, structure, and reactivity of ruthenium(II) complexes with a hemilabile tetradentate etherdiphosphine ligand

Ekkehard Lindner* , Joachim Wald, Klaus Eichele, Riad Fawzi¹

Institut für Anorganische Chemie der Universität Tübingen, Eberhard-Karls-Universität, Auf der Morgenstelle 18, D-72076 Tübingen, Germany

Received 22 December 1999

Abstract

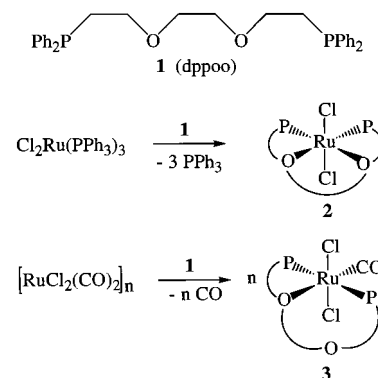
In refluxing toluene the tetradentate ligand $(\text{Ph}_2\text{PCH}_2\text{CH}_2\text{OCH}_2)_2$ (**1**) reacts with $\text{Cl}_2\text{Ru}(\text{PPh}_3)_3$ to give the stable η^4 - (O,O,P,P) -chelated ruthenium(II) complex *trans*- $\text{Cl}_2\text{Ru}(\text{Ph}_2\text{PCH}_2\text{CH}_2\text{OCH}_2)_2$ (**2**). With carbon monoxide no transformation to an η^3 - (O,P,P) - or η^2 - (P,P) -chelated complex accompanied by an uptake of CO takes place. However, if $[\text{Cl}_2\text{Ru}(\text{CO})_2]_n$ is treated with **1** in a mixture of dichloromethane and 2-methoxyethanol, the η^3 - (O,P,P) -coordinated ruthenium(II) complex *trans*- $\text{Cl}_2\text{Ru}(\text{CO})(\text{Ph}_2\text{PCH}_2\text{CH}_2\text{OCH}_2)_2$ (**3**) is formed. Attempts to eliminate carbon monoxide from complex **3** to give **2** failed. Also, **3** does not react with further carbon monoxide to form an η^2 - (P,P) -chelated dicarbonylruthenium(II) complex. Complexes **2** and **3** have been characterized by X-ray structural analyses. © 2000 Elsevier Science S.A. All rights reserved.

Keywords: Ruthenium complexes; Tetradentate ether–phosphine ligands; Crystal structures

1. Introduction

Ether–phosphines belong to the group of hemilabile ligands and have attracted considerable interest in recent years [1–4]. They are equipped with a soft phosphorus and a hard oxygen donor function. Whereas the phosphorus atom is strongly coordinated to a late transition-metal center, the ether oxygen atom forms only a weak contact to this metal. Therefore, the ether moiety behaves like an intramolecular solvent being easily replaced by an incoming substrate [5]. Additionally, the oxygen function is able to stabilize coordinatively unsaturated transition-metal fragments, an important feature in catalysis [6]. The reversible protection of one or more coordination sites by an intramolecular solvent is the most important property of hemilabile ligands like ether–phosphines, which often leads to an improvement in both catalytic and organometallic model reactions. It has to be considered that the ability of the weakly coordinated ether function to afford empty coordination sites is also con-

trolled by steric and conformational factors of the ligand backbone. Obviously this is the reason why in the complex chemistry with hemilabile ligands in most cases a direct connection between the oxygen donors was avoided [7]. Recently however, Mathieu and co-workers reported on a bis(diphenylphosphino)-3,6-dioxaoctane complex of rhodium(I) showing some catalytic activity in the hydroformylation of 1-hexene [8]. The present investigation reports on the first η^3 - and η^4 -coordinated ruthenium(II) complexes with this ligand and their behavior toward carbon monoxide.



Scheme 1.

* Corresponding author. Tel.: +49-7071-2972039; fax: +49-7071-295306.

E-mail address: ekkehard.lindner@uni-tuebingen.de (E. Lindner)

¹ Deceased.

2. Results and discussion

2.1. Synthesis of η^4 - and η^3 -dppoo complexes of ruthenium(II)

If $\text{Cl}_2\text{Ru}(\text{PPh}_3)_3$ is reacted with one equivalent of the dppoo ligand **1** in boiling toluene, a nearly quantitative reaction takes place and the thermally rather stable (η^4 -dppoo)ruthenium(II) complex **2** precipitates as an orange–brown solid if the reaction mixture is cooled to ambient temperature (Scheme 1). Compound **2** dissolves readily in organic solvents of medium polarity (e.g. dichloromethane, chloroform). The composition of **2** was established by a FD mass spectrum, revealing the molecular peak at $m/z = 658$. A singlet in the $^{31}\text{P}\{^1\text{H}\}$ -NMR spectrum of **2** (in CD_2Cl_2) points to the equivalence of both phosphorus atoms and the chemical shift of 66.3 ppm is typical for five-membered rings which means that the ligand **1** is coordinated to ruthenium(II) in an η^4 -fashion. In agreement with this observation the ^1H and ^{13}C signals of the oxygen adjacent methylene groups in the ^1H - and $^{13}\text{C}\{^1\text{H}\}$ -NMR spectra of **2** are also shifted to lower field compared to **1**.

A typical reaction for ruthenium(II) and other transition-metal complexes containing at least two bidentate $\eta^2(\text{O},\text{P})$ -chelated ether–phosphine ligands [9] is the consecutive cleavage of both metal–oxygen bonds in the presence of small donor molecules like sulfur dioxide, carbon disulfide, nitriles or isonitriles, phenylacetylene or carbon monoxide. Since dppoo (**1**) represents formally the combination of two bidentate O,P ligands in the ruthenium(II) complex **2**, a similar reactivity toward such small molecules should be expected. However, if a solution of $[\text{Cl}_2\text{Ru}(\eta^4\text{-dppoo})]$ (**2**) in CH_2Cl_2 is subjected to an atmosphere of carbon monoxide at ambient temperature, no transformation from an η^4 - to an η^3 - or η^2 -complex accompanied by a concomitant uptake of CO takes place. Therefore, the behavior of **1** toward $[\text{Ru}(\text{CO})_2\text{Cl}_2]_n$ was investigated. In a mixture of dichloromethane and 2-methoxyethanol both starting materials were reacted in a 1:1 ratio at room temperature under high dilution conditions to avoid the formation of bridged oligomeric products [10]. After work-up of the reaction mixture, the yellow η^3 -dppoo coordinated ruthenium(II) complex **3** was obtained (Scheme 1). It dissolves readily in chlorinated hydrocarbons and is thermally rather stable. The FAB mass spectrum of **3** displays a molecular peak at $m/z = 686$. In the IR spectrum of **3** (KBr) an intense absorption at 1934 cm^{-1} is observed, which is ascribed to the carbonyl ligand. The location of this band is characteristic for a *trans* position to an ether oxygen function. The $^{31}\text{P}\{^1\text{H}\}$ -NMR spectrum of **3** (in CD_2Cl_2) reveals only a signal at room temperature (δ 34). Obviously a rapid exchange between both oxygen donors in the coordination sphere of ruthenium(II) takes place [7b]. To cor-

roborate this dynamic behavior the temperature was gradually decreased. First, a broadening of the ^{31}P signal takes place, then it disappears at -70°C . The metal–oxygen contact is also indicated in the $^{13}\text{C}\{^1\text{H}\}$ -NMR spectrum of **3**. The ^{13}C signals of the methylene groups that are in the vicinity of the ether oxygen donor are shifted to lower field. Carbon nuclei adjacent to phosphorus show signals appearing as pseudo triplets. Their signals correspond to the X part of an ABX spin system [11]. The intensity ratio of the central line and the two N lines indicates that the coupling between the two phosphorus nuclei is much stronger than anticipated for typical $^2J(\text{P},\text{P})_{\text{cis}}$ coupling constants [7b], suggesting a *trans* arrangement of both phosphorus atoms.

Attempts to eliminate carbon monoxide from complex **3** by heating the yellow solid over a period of about 16 h at 90°C failed [12]. If a solution of **3** in CH_2Cl_2 is treated with carbon monoxide at room temperature or under more drastic conditions (60 bar, 60°C , 24 h) in an autoclave [12], the reaction does not proceed selectively to one product; only a mixture of different (dppoo)ruthenium(II) complexes was obtained.

2.2. Discussion of the X-ray crystal structures of **2** and **3**

The crystal structure of **2** (Fig. 1) is analogous to that of $[\text{Rh}(\text{dppoo})\text{Cl}_2][\text{PF}_6]$ [8]. Selected bond distances and angles are collected in Table 1. Ruthenium is coordinated in an octahedral manner with the η^4 -coordinated dppoo ligand occupying and effectively shielding the equatorial plane. Both chlorine atoms adopt a *trans* arrangement in axial positions. Although the atoms of the equatorial plane, Ru(1), P(1), P(2), O(1), and O(2), deviate by less than 0.07 \AA from the least-squares plane, the in-plane P–Ru–P and O–Ru–O angles, $108.79(8)$ and $74.45(16)^\circ$, respectively, deviate drastically from an ideal octahedral geometry, presumably due to the steric constraints imposed by the three fused five-membered chelate rings. The two chlorine atoms are forced away from their ideal axial positions and are slightly bent towards the oxygen atoms. Altogether, the molecule crystallizes with pseudo C_2 symmetry. This fact is reflected in the conformation of the three five-membered chelate rings: the two outer rings adopt envelope conformations with the tip atoms C(26) and C(29) located about 0.6 \AA above and below their respective ring planes, while the center chelate prefers a twist conformation with C(27) and C(28) being 0.31 and 0.46 \AA below and above the O(1)–Ru(1)–O(2) plane. The flap angle of both envelope conformations lies at about 135° .

In **3**, the η^3 -coordination mode of the dppoo ligand results in the formation of a bicyclic system. Ruthenium

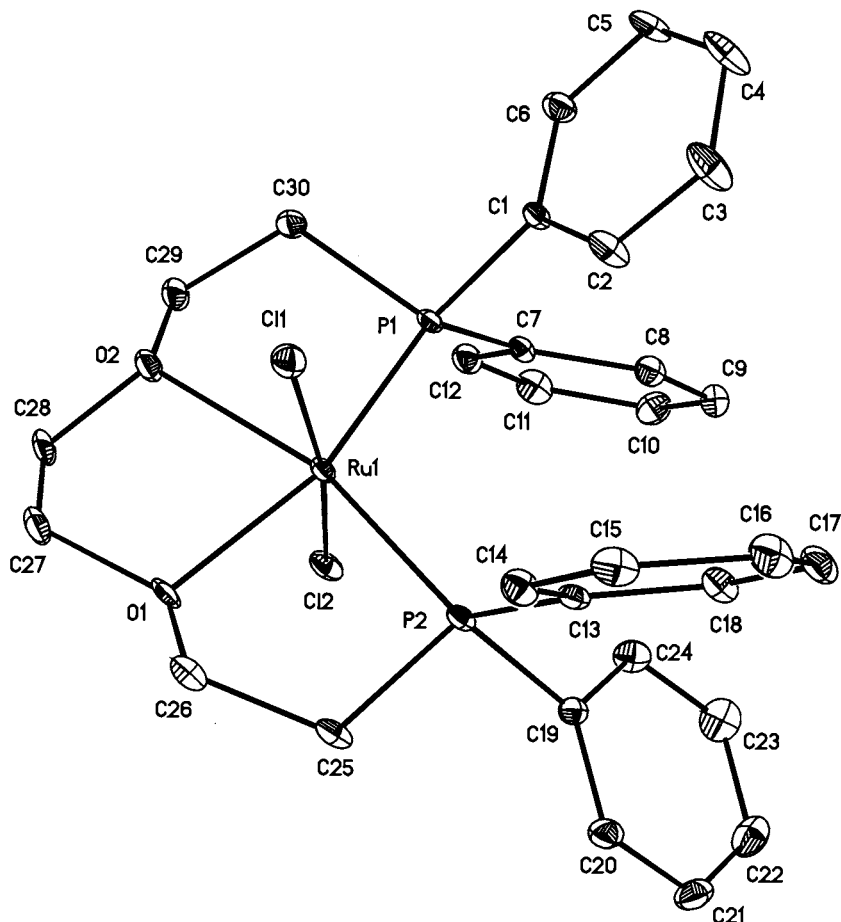


Fig. 1. ORTEP plot of the molecular structure of compound **2**. Thermal ellipsoids are drawn at 20% probability level, except for H atoms. Solvent molecules are omitted for clarity.

and the coordinated ether oxygen are the bridgeheads of the annealed rings and connect a five- and eight-membered ring. The five-membered ring favors a distorted conformation between an envelope and twist conformation, with a C(25)–P(1)–Ru(1)–O(1) torsional angle of 7.5° , and C(25) and C(26) being $-0.25(1)$ and $0.51(1)$ Å below and above the plane defined by Ru(1), P(2), and O(1), respectively. The eight-membered ring adopts a conformation that is uncommon for ring systems of this size: a slightly distorted chair–boat conformation. The two ruthenium–phosphorus bond lengths are equal within error limits. The trigonal geometry of O(1) is slightly distorted; the relatively small Ru(1)–O(1)–C(26) angle of the five-membered ring, $113.1(4)^\circ$, is counterbalanced by an enlarged Ru(1)–O(1)–C(27) angle in the eight-membered ring, $125.5(4)^\circ$. The other oxygen atom of the dppoo ligand, O(2), is with 4.296 Å clearly too remote from the ruthenium to take part in any kind of coordination. The position of the CO group *trans* to the ether oxygen, deduced from IR spectroscopy, is confirmed by the X-ray diffraction data (Fig. 2). Compound **3** is the first complex of dppoo for which

the η^3 -coordination is established by single-crystal X-ray diffraction.

3. Conclusions

Although the tetradentate dppoo ligand **1** is able to coordinate to ruthenium(II) via one or even both oxygen donor functions as demonstrated in the case of complexes **3** and **2**, attempts to activate small molecules like carbon monoxide with cleavage of the weak Ru–O bonds were not successful. This behavior is in marked contrast to corresponding (*O,P*)-bis(chelated) ruthenium(II) complexes containing two bidentate ether–phosphine ligands [7b,9,12]. The main difference between both ligand types is a bridging ethylene function between both ether oxygen donors in **1**. Hence polycyclic chelate rings are formed as soon as one or both oxygen atoms coordinate to ruthenium(II). By this coordination mode not only the mobility of the whole ligand system is reduced, but also the reactive centers are shielded. In this way the cleavage of the Ru–O bonds is impeded and the hemilabile character of the ligand is weakened.

4. Experimental

4.1. General procedures

All manipulations were carried out under an atmosphere of argon by use of standard Schlenk techniques. Solvents were dried with appropriate reagents, distilled, degassed and stored under argon. IR data were obtained with a Bruker IFS 48 FTIR spectrometer. FD mass spectra were taken on a Finnigan MAT 711 A instrument, modified by AMD; FAB mass spectra were recorded on a Finnigan TSQ 70. Elemental analyses were performed with a Carlo Erba 1106 analyzer; Cl analyses were carried out according to Schöniger [13]. ^1H -, $^{31}\text{P}\{^1\text{H}\}$ -, and $^{13}\text{C}\{^1\text{H}\}$ -NMR spectra were recorded on a Bruker DRX 250 spectrometer at 250.13, 101.25, and 62.90 MHz, respectively at 25°C. ^1H and ^{13}C chemical shifts were measured relative to partially deuterated solvent peaks and to deuterated solvent peaks, respectively, which are reported relative to TMS. ^{31}P chemical shifts were measured relative to 85% H_3PO_4 ($\delta = 0$). $^{31}\text{P}\{^1\text{H}\}$ -NMR spectra were also recorded on a Bruker AC 80 instrument operating at 32.44 MHz with external standard. At low temperatures, 0 to -80°C , 1% H_3PO_4 in acetone- d_6 was used as an external standard and above 0°C , 1% H_3PO_4 in D_2O . The temperatures of the variable-temperature $^{31}\text{P}\{^1\text{H}\}$ -NMR spectra were calibrated using the method of van Geet [14] and are considered accurate to ± 1 K. The diphosphine ligand **1** was synthesized according to a procedure published by Dapporto and Sacconi [15].

Table 1
Selected bond lengths (Å) and angles (°) for **2** and **3**

	2 ·H ₂ O	3 ·CH ₂ Cl ₂ ·H ₂ O
<i>Bond lengths</i>		
Ru(1)–Cl(1)	2.393(2)	2.401(3)
Ru(1)–Cl(2)	2.386(2)	2.377(3)
Ru(1)–P(1)	2.135(2)	2.401(2)
Ru(1)–P(2)	2.2689(19)	2.360(2)
Ru(1)–O(1)	2.116(4)	2.207(6)
Ru(1)–O(2)	2.248(4)	
Ru(1)–C(31)		1.828(9)
<i>Bond angles</i>		
O(1)–Ru(1)–O(2)	74.47(16)	
O(2)–Ru(1)–P(2)	163.15(11)	
Cl(2)–Ru(1)–Cl(1)	172.76(5)	172.36(8)
P(1)–Ru(1)–P(2)	108.79(8)	172.55(7)
Cl(2)–Ru(1)–P(1)	90.00(7)	94.88(9)
Cl(1)–Ru(1)–P(1)	93.64(8)	86.06(9)
P(1)–Ru(1)–O(2)	87.96(12)	
C(26)–O(1)–C(27)	117.2(4)	114.2(6)
C(26)–O(1)–Ru(1)	110.6(3)	113.5(4)
C(27)–O(1)–Ru(1)	112.6(3)	125.5(5)
C(29)–O(2)–C(28)	112.1(4)	115.1(6)
C(29)–O(2)–Ru(1)	112.0(3)	
C(28)–O(2)–Ru(1)	112.5(3)	

4.2. *trans*-Dichloro-*cis*-1,8-bis[(diphenylphosphino)-3,6-dioxaocane-*O,O,P,P*]ruthenium(II) (**2**)

To a solution of $\text{Cl}_2\text{Ru}(\text{PPh}_2)_3$ (0.958 g, 1.0 mmol) in 250 ml of boiling toluene a solution of bis-(diphenylphosphino)-3,6-dioxaocane (**1**) (0.486 g, 1.0 mmol) in 150 ml of toluene was added dropwise. To complete the reaction, the mixture was refluxed for 16 h. The solution was cooled to room temperature and **2** precipitated as an orange–brown solid, which was isolated by filtration (P3). Yield: 0.53 g (82%); m.p. 243°C . MS (FD, 35°C): m/z 657.9 [M^+]. Anal. Calc. for $\text{C}_{30}\text{H}_{32}\text{P}_2\text{O}_2\text{RuCl}_2$ (658.405): C, 54.72; H, 4.90; Cl, 10.77%. Found: C, 54.22; H, 4.85; Cl, 10.97%. $^{31}\text{P}\{^1\text{H}\}$ -NMR (101.26 MHz, CDCl_3 , 25°C): $\delta = 66.3$ (s). ^1H -NMR (250.13 MHz, CDCl_3 , 25°C): $\delta = 7.0$ – 7.2 (m, 20H, PPh_2); $\delta = 4.3$ (s, br, 8H, $\text{Ph}_2\text{PCH}_2\text{CH}_2\text{OCH}_2$); $\delta = 3.0$ (s, br, 4H, PPh_2CH_2). $^{13}\text{C}\{^1\text{H}\}$ -NMR (62.90 MHz, CD_2Cl_2 , 25°C): $\delta = 136.1$ (m, $N^2 = 45.5$ Hz [11], $^1J(\text{PC}) = 44$ Hz, $^3J(\text{PC}) = 1.5$ Hz, $^2J(\text{P,P}') = 33$ Hz, *ipso*-C of PPh_2); $\delta = 133.3$ (m, $N^2 = 9.3$ Hz [11], *o*-C of PPh_2); $\delta = 129.0$ (s, *p*-C of PPh_2); $\delta = 126.9$ (m, $N^2 = 10.0$ Hz [11], *m*-C of PPh_2); $\delta = 73.3$ (s, $\text{PPh}_2\text{CH}_2\text{CH}_2\text{OCH}_2$); $\delta = 70.2$ (s, $\text{PPh}_2\text{CH}_2\text{CH}_2\text{OCH}_2$); $\delta = 34.7$ (m, $N^2 = 24.2$ Hz [11], $\text{PPh}_2\text{CH}_2\text{CH}_2\text{OCH}_2$).

4.3. Carbonyl(*trans*-dichloro)-*trans*-1,8-bis[(diphenylphosphino)-3,6-dioxaocane-*O,P,P*]ruthenium(II) (**3**)

$\text{RuCl}_3 \cdot x\text{H}_2\text{O}$ (510 mg, 2.02 mmol) was dissolved in 200 ml of boiling 2-methoxyethanol. Carbon monoxide was bubbled through the refluxing solution for 5 h until the color of the reaction mixture turned to yellow, indicating the formation of the precursor $[\text{Ru}(\text{CO})_2\text{Cl}_2]_n$. Bis(diphenylphosphino)-3,6-dioxaocane (**1**) (980 mg, 2.02 mmol) was dissolved in a mixture of 250 ml of 2-methoxyethanol and of dichloromethane (1:1). Both solutions were transferred in two different dropping funnels and the solutions were added slowly within 6 h under vigorous stirring to a reaction vessel charged with 500 ml of dichloromethane. To complete the reaction, the mixture was stirred for 16 h at ambient temperature. After the solvent mixture was removed under reduced pressure, the remainder was dissolved in 50 ml of dichloromethane. The product precipitated by the addition of 25 ml of *n*-pentane and was collected by filtration (P3). Yield: 1.05 g (76%) of **3**, yellow powder; decomposition 225°C ; MS (FAB, 30°C): m/z 686.0 [M^+], 651.1 [$\text{M}^+ - \text{Cl}$], 587.2 [$\text{M}^+ - 2\text{Cl} - \text{CO}$]. Anal. Calc. for $\text{C}_{31}\text{H}_{32}\text{P}_2\text{O}_3\text{RuCl}_2$ (686.514): C, 54.23; H, 4.69; Cl, 10.32%. Found: C, 53.87; H, 4.74; Cl, 10.43%. IR (KBr): $\nu(\text{CO}) = 1934$ cm^{-1} . $^{31}\text{P}\{^1\text{H}\}$ -NMR (101.26

² X part of an ABX spin system, $N = |^mJ(\text{AX})| + |^nJ(\text{BX})|$.

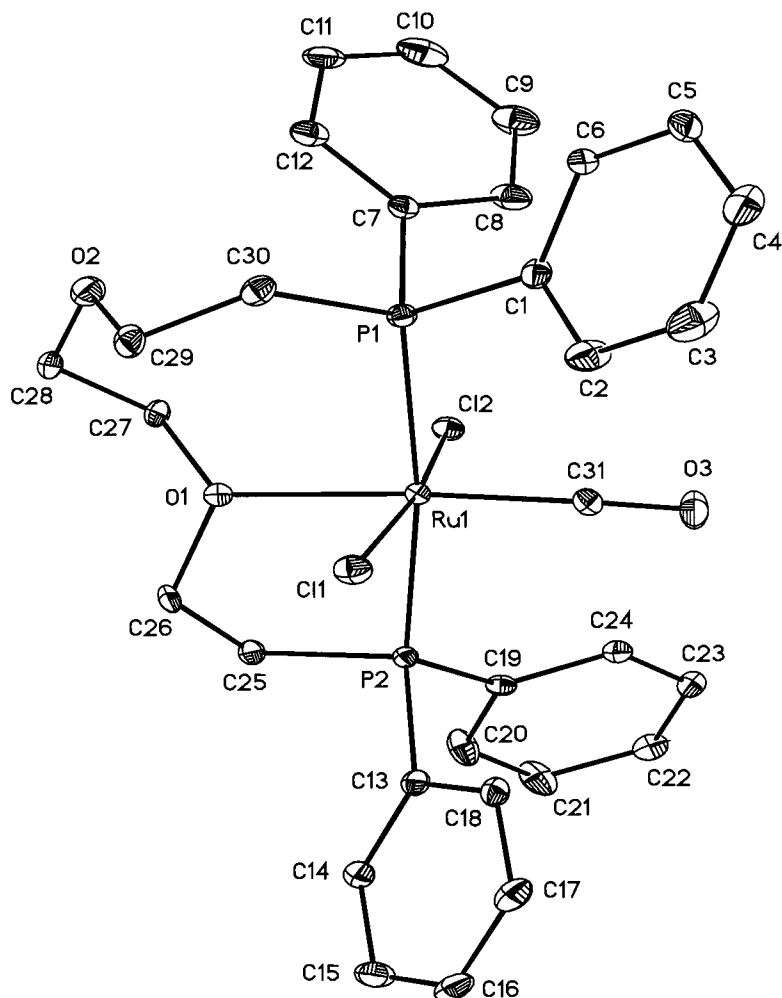


Fig. 2. ORTEP plot of the molecular structure of compound **3**. Thermal ellipsoids are drawn at 20% probability level, except for H atoms. Solvent molecules are omitted for clarity.

MHz, CD_2Cl_2 , 25°C): $\delta = 34.0$ (s). $^{13}\text{C}\{^1\text{H}\}$ -NMR (62.90 MHz, CD_2Cl_2 , 25°C): $\delta = 131.6$ (m, $N^1 = 46.2$ Hz [11], *ipso*-C of PPh_2); $\delta = 132.5$ (m, $N^1 = 10.6$ Hz [11], *o*-C of PPh_2); $\delta = 127.1$ (m, $N^1 = 9.9$ Hz [11], *m*-C of PPh_2); $\delta = 129.0$ (m, $N^1 = 2.8$ Hz [11], *p*-C of PPh_2); $\delta = 81.4$ (s, $\text{PCH}_2\text{CH}_2\text{OCH}_2$); $\delta = 72.4$ (s, $\text{PCH}_2\text{CH}_2\text{OCH}_2$); 26.4 (m, $N^1 = 24.9$ Hz [11], $\text{PCH}_2\text{CH}_2\text{OCH}_2$).

4.4. Single-crystal X-ray diffraction analyses

Crystals of **3** were grown from a mixture of dichloromethane and ethyl acetate (1:4). Data for **2** and **3** were collected on a Siemens P4 diffractometer operating in the ω scan mode, using graphite monochromated Mo- K_α radiation ($\lambda = 0.71073$ Å). Full details of crystal data, data collection and structure refinement are given in Table 2. The structures were solved by direct methods and refined by full-matrix least-squares on F^2

using Bruker SHELXTL 5.10. Non-hydrogen atoms were refined with anisotropic displacement parameters, except for the atoms of the solvent molecules. Hydrogen atoms were constrained to idealized positions using a riding model (with free rotation for methyl groups). Solvent molecules present in crystals of both **2** and **3** were disordered and not clearly defined and hence refined isotropically. The largest difference peak and holes are located less than 1 Å away from ruthenium.

5. Supplementary material

Crystallographic data for the structural analysis has been deposited with the Cambridge Crystallographic Data Center, CCDC nos. 137576 for compound **2** and 137575 for complex **3**. Copies of this information may be obtained free of charge from The Director, CCDC,

Table 2
Crystal data and structure refinement details for complexes **2** and **3**

	2·H ₂ O	3·CH ₂ Cl ₂ ·H ₂ O
Empirical formula	C ₃₀ H ₃₄ Cl ₂ O ₃ P ₂ Ru	C ₃₂ H ₃₆ Cl ₄ O ₄ P ₂ Ru
Formula weight	676.48	789.42
Crystal color	Orange-brown	Yellow
Crystal size (mm)	0.50 × 0.35 × 0.10	0.31 × 0.24 × 0.11
Unit cell dimensions		
<i>a</i> (Å)	10.285(6)	14.602(9)
<i>b</i> (Å)	10.296(6)	12.739(9)
<i>c</i> (Å)	16.334(11)	18.143(14)
α (°)	84.52(6)	90
β (°)	71.84(4)	91.81(6)
γ (°)	63.80(4)	90
Crystal system	Triclinic	Monoclinic
Space group	<i>P</i> $\bar{1}$	<i>P</i> 2 ₁ / <i>c</i>
<i>Z</i>	2	4
Temperature (K)	173(2)	173(2)
Reflections collected/unique	13 514/6757	11 813/5943
<i>R</i> _{int}	0.0582	0.1142
Limiting indices <i>hkl</i>	–13–13, –13–13, –21–21	–17–17, –15–0, –21–21
θ Range for data collection (°)	2.21–28.94	2.12–25.03
Completeness to θ (%)	87.0	99.7
Absorption coefficient (mm ^{–1})	0.853	0.912
Absorption correction	None	ψ scans
Max./min. transmission		0.541/0.475
Data/restraints/parameters	6757/0/338	5943/0/369
Goodness-of-fit on <i>F</i> ²	1.114	0.944
Final <i>R</i> indices [<i>I</i> > 2 σ (<i>I</i>)], <i>R</i> ₁ / <i>wR</i> ₂	0.0706 ^a /0.1741 ^b	0.0737 ^a /0.1925 ^b
<i>R</i> indices (all data), <i>R</i> ₁ / <i>wR</i> ₂	0.0857 ^a /0.1851 ^b	0.1070 ^a /0.2124 ^b
Extinction coefficient	0.0003(10)	0.0000(3)
Largest diff. peak and hole (e Å ^{–3})	2.107, –3.010	1.802, –1.226

$$^a R_1 = \frac{\sum ||F_o| - |F_c||}{\sum |F_o|}$$

$$^b wR_2 = \left[\frac{\sum [w(F_o^2 - F_c^2)^2]}{\sum [w(F_o^2)^2]} \right]^{0.5}$$

12 Union Road, Cambridge, CB2 1EZ, UK (Fax: +44-1223-336033; e-mail: deposit@ccdc.cam.ac.uk or www:http://www.ccdc.cam.ac.uk).

Acknowledgements

Support of this research by the Fonds der Chemischen Industrie is gratefully acknowledged. K.E. appreciates discussions with Dr Christiane Nachtigal.

References

- [1] J.C. Jeffrey, T.B. Rauchfuss, *Inorg. Chem.* 18 (1979) 2658.
- [2] A. Bader, E. Lindner, *Coord. Chem. Rev.* 108 (1991) 27.
- [3] E. Lindner, S. Pautz, M. Hausteine, *Coord. Chem. Rev.* 155 (1996) 145.
- [4] (a) H. Yang, M. Alvarez-Gressier, N. Lugan, R. Mathieu, *Organometallics* 16 (1997) 1401. (b) P. Braunstein, Y. Chauvin, J. Nahring, A. Decian, J. Fischer, A. Tiripicchio, F. Ugozzoli, *Organometallics* 15 (1996) 5551. (c) S.J. Chadwell, S.J. Coles, P.G. Edwards, M.B. Hurthouse, *J. Chem. Soc. Dalton Trans.* (1996) 1105. (d) T.B. Higgins, C.A. Mirkin, *Inorg. Chim. Acta* 240 (1995) 347. (e) T. Braun, P. Steinert, H. Werner, *J. Organomet. Chem.* 488 (1995) 169. (f) H. Werner, A. Stark, P. Steinert, G. Grünwald, J. Wolf, *Chem. Ber.* 128 (1995) 49.
- [5] (a) E. Lindner, M. Hausteine, R. Fawzi, M. Steimann, P. Wegner, *Organometallics* 13 (1994) 5021. (b) E. Lindner, M. Hausteine, H.A. Mayer, K. Gierling, R. Fawzi, M. Steimann, *Organometallics* 14 (1995) 2246. (c) E. Lindner, S. Pautz, M. Hausteine, *J. Organomet. Chem.* 509 (1996) 215.
- [6] (a) E. Lindner, B. Keppeler, H.A. Mayer, K. Gierling, R. Fawzi, M. Steimann, *J. Organomet. Chem.* 526 (1996) 175. (b) E. Lindner, B. Keppeler, P. Wegner, *Inorg. Chim. Acta* 258 (1997) 97.
- [7] (a) E. Lindner, J. Dettinger, H.A. Mayer, H. Kühbauch, R. Fawzi, M. Steimann *Chem. Ber.* 126 (1993) 1317. (b) E. Lindner, A. Möckel, H.A. Mayer, H. Kühbauch, R. Fawzi, M. Steimann, *Inorg. Chem.* 32 (1993) 1266. (c) E. Lindner, M. Hausteine, H.A. Mayer, H. Kühbauch, K. Vrieze, B. de Klerk-Engels, *Inorg. Chim. Acta* 215 (1994) 165.
- [8] M. Alvarez, N. Lugan, R. Mathieu, *J. Organomet. Chem.* 468 (1994) 249.
- [9] E. Lindner, M. Geprägs, K. Gierling, R. Fawzi, M. Steimann, *Inorg. Chem.* 34 (1995) 6106.
- [10] L. Rossa, F. Vögtle, in: F. Vögtle (Ed.), *Synthesis of Medio- and Macrocyclic Compounds by High Dilution Principle Techniques: Topics in Current Chemistry*. Cyclophanes I, vol. 113, Springer, Heidelberg, 1983.
- [11] R.K. Harris, *Can. J. Chem.* 42 (1964) 2275.
- [12] E. Lindner, U. Schober, R. Fawzi, W. Hiller, U. Englert, P. Wegner, *Chem. Ber.* 120 (1987) 1621.
- [13] W. Schöniger, *Microchim. Acta* (1955) 123.
- [14] A.L. van Geet, *Anal. Chem.* 40 (1968) 2227.
- [15] P. Dapporto, L. Sacconi, *J. Chem. Soc. A* (1971) 1914.